JACS
JOURNAL OF THE AMERICAN CHEMICAL SOCIETY
Communication
pubs.acs.org/JACS

Shock Wave Chemistry in a Metal–Organic Framework

Zhi Su,[†] William L. Shaw, Yu-Run Miao, Sizhu You, Dana D. Dlott,* and Kenneth S. Suslick*

Department of Chemistry, University of Illinois at Urbana–Champaign, Urbana, Illinois 61801, United States

Supporting Information

ABSTRACT: Metal–organic frameworks (MOFs) have potential applications as energy absorbing materials for shock wave energy mitigation due to their nanoporosity. Here we have examined km/s laser-driven flyer plate impacts on a prototypical MOF, ZIF-8. We observed particle fragmentation and morphological changes in microcrystals of ZIF-8 at lower shock pressures (≈2.5 GPa), and amorphization and structural collapse at higher pressures (≈8 GPa). High-speed emission spectroscopy revealed that 50 ns after flyer plate impacts, an emission pulse was generated by ZIF-8 resulting from chemical bonds that were broken and subsequently reformed. MOFs may prove useful in the dissipation of shock wave energy through large structural changes (free volume collapse and endothermic bond breakage).

The shock waves generated by explosives or by high velocity objects are a serious hazard both to personnel and to equipment.[1] As such, there is keen interest in developing new mechanisms for shock-protective materials.[2] In this study, we investigated whether it might be possible to incorporate shock-absorbing chemical functionality in the form of nanoporous materials. Many shock absorbing materials (such as sand or foam) function by compactification of void spaces.[2a,3] By extending this mechanism down to the nm scale, we may be able to protect against shocks by using their energy to drive otherwise harmless endothermic chemical reactions: this would weaken the shock by absorbing its energy and attenuating its effects by stretching out the remaining energy in time. Based on what is known about detonations, where exothermic chemistries sustain a shock wave, in attenuation we would expect the initial bond-breaking endothermic steps to happen promptly behind the shock front, whereas the chemically stored shock energy would be released more gradually, as heat, as broken bonds reform.[4]

To this end, we have examined the effects of shock on an archetypal metal–organic framework material (MOF) in the hope that shock compression might also break massive numbers of chemical bonds, and indeed that proves to be true. For our initial studies, we chose a well-known MOF, ZIF-8 (zeolitic imidazolate framework), as the target material because its excellent chemical and thermal stability permitted desolvation without structural collapse.[5] The ZIF-8 framework is constructed of Zn(II) ions coordinating four bridging 2-methylimidazolate (2-MeIm) ligands and has ≈50% internal free volume (Figure 1). Our ZIF-8 samples consisted of thin layers of polymer-bonded microcrystals (Supporting Information (SI), Figures S1 and S2)[5b] of the nanoporous ZIF-8, which itself is constructed of Zn(II) ions coordinating four bridging 2-methylimidazolate (2-MeIm) ligands (Figure 1a). Our working hypothesis was that this material would react to shock compression by collapse of the nanopores and consequent endothermic chemical reactions involving massive (and sudden) cleavage of the coordination bonds and perhaps other bonds of the ZIF framework.

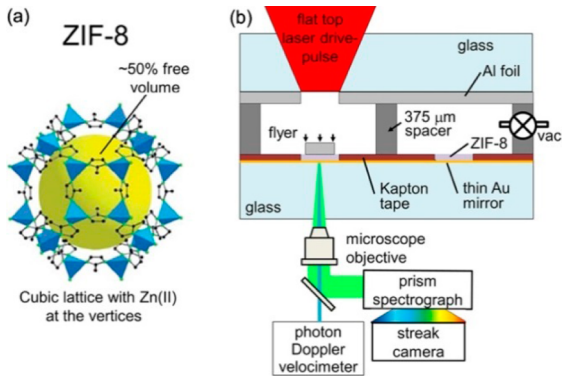

Figure 1. (a) Structure of ZIF-8. (b) Microflyer plate apparatus with shock-induced emission/photoemission monitoring. The flyer plates generate a well-defined 16 ns duration planar shock in the ZIF-8 sample which coats a thin (150 nm) gold mirror on a Pyrex substrate.

MOFs encompass a wide range of forms and functionalities that might be exploited and optimized for shock protection. They can have extremely high surface areas with tunable porosities and variable chemical and physical properties.[7] Their mechanical, chemical, and thermal stabilities are critical to their use in applications, and it is important to understand the requirements necessary to provide structural integrity and porosity after removal of solvates.[8]

The effects of shock compression on nanoporous materials, however, are still only poorly understood. To date, studies of the mechanical properties of MOFs have been primarily of static or quasistatic compression by utilization of diamond anvil cell (DAC)[9] or nanoindentation[10] (which is more controllable and less destructive). Under quasistatic compression, individual ZIF-8 microcrystals can maintain their porous structure up to around 2 GPa, but by 4 GPa those crystals lost ≈60% of their initial volume.[6]

Shock compression (ranging from a simple hammer blow to a km/s impact or a nearby explosion), however, has been only rarely examined for its effects on MOFs: the one prior example involved gas-gun fired flyer plates that produced pressures of 0.3 to 7.5 GPa on Cu-BTC (BTC = 1,3,5-benzenetricarboxylate) framework solid.[11] After-shock evaluations of crystallinity using

Received: December 16, 2016

DOI: 10.1021/jacs.6b12956
J. Am. Chem. Soc. XXXX, XXX, XXX–XXX

powder X-ray diffraction (PXRD) found that MOF structural stability toward shock was enhanced by inclusion of ferrocene in the pores; no further analysis of the nature or dynamics of structural changes was presented.

In the experiments reported here, shocks in the MOFs were created by impacts with thin Al flyer plates moving at km/s velocities (1 km/s = 1 μm/ns), producing GPa pressures (1 GPa = 10 000 bar). Our tabletop shock compression spectroscopy apparatus uses a pulsed laser to launch a 75 μm thick Al foil at the sample generating a 16 ns steadily driven shock via 0−1.6 km/s planar impacts (Figure 1b and Experimental details in SI).[12] In some postmortem measurements, we used 25 μm flyers, that produced ∼4 ns duration shocks with impact velocities up to 4 km/s. Thin films of desolvated MOF microcrystals[5b] mounted on a glass substrate (SI, Figures S1 and S2) with an 40 nm Au mirror coating were shocked using laser-driven 25 μm thick Al flyer plates to impact the MOF at velocities of up to 4 km/s (cf. SI for experimental details).[12] The flyer plate velocity history during flight and impact was characterized by photon Doppler velocimetry (PDV). When the flyer plate struck the MOF, it launched a shock wave that propagated through the MOF, past the Au mirror and into the glass. PDV monitored the shape of the transmitted shock, beginning from the instant it exited the MOF layer with 2 ns time resolution.

Optical microscopic images taken before and after flyer impacts show clearly defined impact craters (Figure 2 and SI S1).

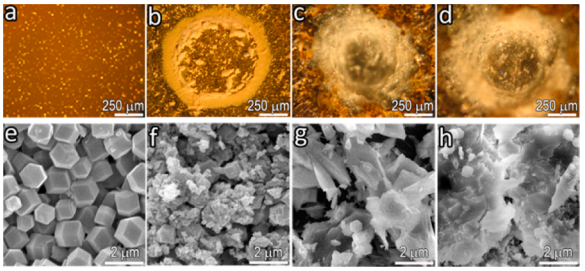

Figure 2. Optical images (a−d) of ZIF-8 layer on glass substrate and SEM images (e−h) of ZIF-8 crystals after shock compression: (a, e) without shock; (b, f) 0.75 km/s (2.5 GPa), (c, g) 1.3 km/s (5 GPa), and (d, h) 1.6 km/s (8 GPa).

At 0.75 km/s, the coated thin gold layer was not destroyed and the glass substrate kept its integrity; above 1.3 km/s, however, the gold layer and glass substrate were damaged.

Scanning electron microscopy (SEM) was used to examine shock effects on the ZIF-8 layer. SEM indicated that an irreversible morphological change was induced by flyer impact (Figure 2e−h). The ZIF-8 crystals had rhombic dodecahedral morphology with average size around 1.2 μm. After 0.8 km/s impacts, the ZIF-8 crystals were crushed and fragmented. At higher velocities up to 1.6 km/s, the shocked crystals appeared to result from fragmentation and agglomeration or sintering. These morphological changes were irreversible.

To understand these results better, we examined the powder X-ray diffraction (PXRD) of the ZIF-8 samples after shock. At 0.75 km/s, the shocked material had the same major diffraction peaks as the unshocked ZIF-8 crystals, but with significant broadening and loss of intensity (Figure 3). This suggests that at 0.75 km/s, the long-term order of ZIF-8 structure was mostly maintained, but the broadened peaks indicate that both the ZIF-8 crystal particle size and crystallinity were substantially decreased, which is consistent with SEM images. If we compare the PXRD spectra

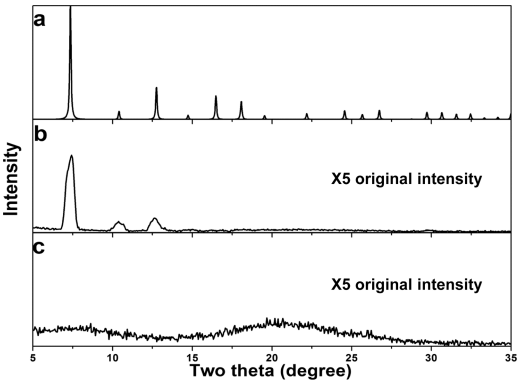

Figure 3. PXRD for ZIF-8 crystals (a) without flyer plate impact, (b) after 0.75 km/s impact, and (c) after 1.3 km/s impact. For clarity, the PXRD intensity for b and c was magnified 5-fold.

of the 2.5 GPa shocked crystals to a sample exposed to 2 GPa static compression generated by a hydraulic piston pelletizer under vacuum,[6] much more damage and much greater amorphization was observed after the static compression. After 2 GPa static compression, PXRD showed nearly complete amorphization with only one highly broadened and weakened peak at 6.6° corresponding to the Zn−2-MeIm−Zn unit.[6] The lesser effect of dynamic compression is likely the result of the vastly different time scales, nanoseconds for the shock vs minutes for the hydraulic piston under vacuum and to additional shear forces created in the piston compression. Complete amorphization of ZIF-8 crystals can be achieved by dynamic compression at 1.3 km/s, corresponding to ≈5 GPa: the diffraction pattern in Figure 3c showed the absence of any sharp diffraction peaks.

Postmortem infrared (IR) absorption spectra offer additional information about shock-induced structural changes in ZIF-8.[13] The spectrum of initially desolvated ZIF-8 was consistent with results previously reported in the literature (Figure 4a). The major IR bands (1800−650 cm^{-1}) were associated with the ligand's methyl group and the imidazole ring.[13a,14] The band at 1580 cm^{-1} was ascribed to conjugated double bond (C═N or C═C) ring stretching, and the complicated bands in the range of 1350−1500 cm^{-1} were assigned to other ring stretches. The bands in the 900−1350 cm^{-1} region and below 800 cm^{-1} have

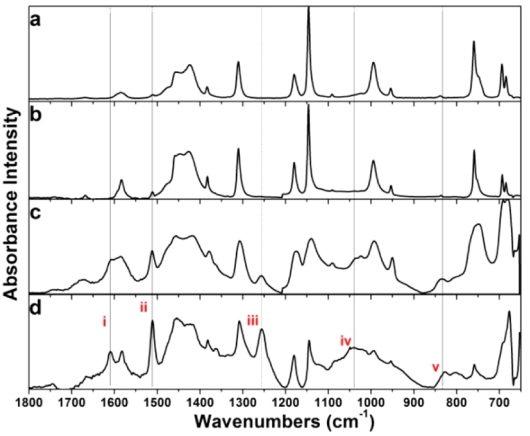

Figure 4. IR spectra of ZIF-8 crystals (a) without impact, and after dynamic compression at (b) 0.75 km/s (2.5 GPa), (c) 1.3 km/s (5 GPa), and (d) 1.6 km/s (8 GPa). The vertical lines indicate the new peaks generated by shock compression. Peaks i, ii, and iii, iv, and v are all associated with lowered symmetry of the 2-MeIm.[15]

DOI: 10.1021/jacs.6b12956
J. Am. Chem. Soc. XXXX, XXX, XXX−XXX

been associated with the in-plane and out-of-plane bending of imidazole rings, respectively.

After shock compression at 0.75 km/s, Figure 4b, the IR spectrum was only slightly different from the unshocked spectrum, suggesting that with these lower-pressure impacts, the ZIF-8 molecular structure and coordination of the imidazolate bridges to the Zn ions was maintained despite severe damage to the crystal morphology, consistent with the PXRD (Figure 3b). With increased velocity impacts (1.3 km/s, Figure 4c), broadened IR peaks were observed, which indicate that site-to-site variations among the 2-methylimidazolates in the solid were generated, presumably due to distortion of the local structure and loss of long-range order. Even so, at 1.3 km/s, ZIF-8 maintained most of its local chemical coordination environment, even though its long-range order had been completely destroyed, as shown in the PXRD, Figure 3c.

After the highest-velocity impacts at 1.6 km/s (Figure 4d), several new absorption bands were observed (1608, 1510, 1257, 1040, and 830 cm^{-1}), some of which may represent splitting of bands from unshocked ZIF-8 (Figure 4d). ZIF-8 crystallizes in the highest symmetry space group (cubic, I_{-43m}); the PXRD shows complete amorphization of ZIF-8 after strong shock compression (Figure 3c). The new peaks in the IR indicate the chemical environment of the ligands was changed significantly and the higher symmetry of ZIF-8 was at least partially lost. For example, the split peak around 1600 cm^{-1} (peak i, Figure 4d) suggests a lowered symmetry of the vibrational modes of imidazole ring conjugated double bonds; as another example, the new band at 1510 cm^{-1} (peak ii, Figure 4d) reflects a lowered symmetry and coupling of the imidazole ring stretching modes to ring-CH and CH_3 deformations.[15] The new band at 1257 cm^{-1} (peak iii, Figure 4d) is consistent with the ring-methyl stretch not normally seen with high symmetry 2-MeIm ligation, but is observed with lower symmetry 4-methyimidazolate ligation,[15] which is again consistent with shock destruction of the high-symmetry structure. In addition, the two new bands at 1040 and 830 cm^{-1} (peaks iv and v, Figure 4d) are associated with lowered-symmetry imidazole rings.[15]

One may also make an interesting comparison of the IR spectra of highly symmetric bridging 2-methylimidazolate ligands vs lowered symmetry environments. The FT-IR spectra of uncompressed ZIF-8 and one-dimensional Ag (I)-2-MeIm coordination polymer (SI Figures S4b vs S4c) are very similar.[16] In contrast, the increased complexity of the shock-compressed ZIF-8 IR spectrum compares to the lowered symmetry of the nonligated 2-methylimidazole (2-MeImH), as shown in SI Figure S4a vs S4d.

To compare the effects of static vs dynamic compression, a diamond anvil cell (DAC) was utilized to generate ≈7 GPa hydrostatic compression of ZIF-8 crystals (SI Figure S5) using Ar as the pressure medium. Under this static compression, all the absorbance bands were blue-shifted about 30 cm^{-1} and pressure-broadened (SI Figure S5b). Upon release of the static compression, the IR spectrum reverted almost entirely back to the uncompressed ZIF-8 spectrum (SI Figure S5c), which suggests little permanent structural change occurred under hydrostatic compression in the DAC up to 7 GPa in the presence of pressurized Ar permeating the porous ZIF-8. This contrasts with the effects of shock compression at nearly the same pressure (8 GPa), where permanent structural changes were observed in the IR spectra. It appears that shock compression was more destructive than static compression in the region of 7−8 GPa: an irreversible change by shock compression vs a reversible change after static compression.

To investigate further the dynamic effects of shock impact on ZIF-8, we also used emission spectroscopy with a fast photomultiplier tube and digitizer to investigate the mechanistic details of MOF shock compression. We did two kinds of experiments (Figures 5, S6−S7). In the in situ photoluminescence (PL) experiments, the MOF was excited with a 150 ns duration laser pulse at 351 nm with and without the impact of flyer plate. In the shock-induced emission measurements, we detected the light produced during and after the impact, without any photoexcitation.

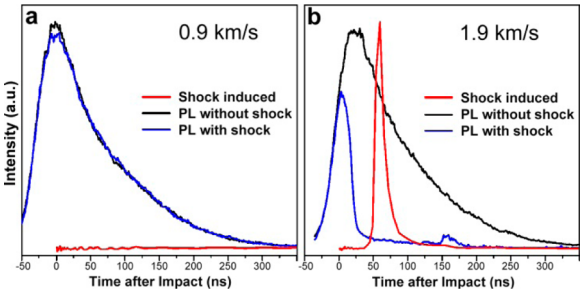

Figure 5. Time-resolved in situ photoluminescence (PL) of ZIF-8 film excited by a florescence pump laser at 350 nm laser pulses with (blue) or without (black) a shock, and shock-induced emission without photoexcitation (red). Time zero denotes flyer plate impact at the ZIF-8 film. Intensities were wavelength-integrated from 400 to 700 nm. The PL duration without shock reflects only the excitation pulse duration.

For the PL measurements, we looked at the emission around 460 nm, which has been assigned to the $\pi-\pi^*$ transition of 2-MeIm ligand in ZIF-8.[13b] At velocities <1.6 km/s, the PL (whose time dependence tracked the 150 ns excitation pulses) was unaffected by shock (Figure 5a), which implies no significant structural changes to ZIF-8 under weak shocks, consistent with the results of PXRD and IR, and there was no emission produced by the shock itself (e.g., Figure 5a). At velocities >1.6 km/s (e.g., Figure 5b), the PL abruptly terminated when the flyer impacted, consistent with the major structural changes occurring under high velocity shock impact. The shock-induced emission was weak with 0.75 km/s impacts, but with 1.6 km/s impacts, an intense shock emission burst lasting 20 ns appeared (Figure 5b): notably, the emission burst did not appear during the shock; instead, it appeared 50 ns after impact. The intensity of this delayed emission burst increased with flyer velocity.

The disappearance of PL after impact indicates a shock-induced chemical process that destroyed the emitting species, whose precise nature remains under investigation. The appearance of a shock-induced emission burst at 50 ns, long after the shock ended, demonstrates that this burst was not triboluminescence created by charge separation during fracture. Instead, the delayed emission from 50 to 100 ns is associated with highly exothermic recombination of the energetic chemical species produced by shock-induced bond scission. The delayed recombination (i.e., bond reformation) occurs in the damaged ZIF structure created by shock-induced collapse of the porous structure, which cannot return to the initial well-ordered ZIF-8 structure. The 50 to 100 ns delayed emission is a clear demonstration that the 1.6 km/s impact created a massive concentration of reactive high-energy chemical species.

Shock-induced emission, of course, has been previously reported in inorganic and organic materials.[17] Photoemission, quite generally, occurs during or promptly after the shock with a

DOI: 10.1021/jacs.6b12956
J. Am. Chem. Soc. XXXX, XXX, XXX−XXX

wide range of solids.[18] In our case, however, the observed emission were long delayed after the shock impact as a result of slow recombination of energetic species formed during the bond scission of the ZIF-8 structure.

Shock mitigation is a new potential application for microporous materials, and MOFs specifically provide a diversity of controllable structures. ZIF-8 is a compact structure comparing to most other MOFs, due to the short bridging ligand (2-MeIm) and single zinc ion center. The use of MOFs with longer bridges and larger pores are likely to show even greater ability to absorb shock wave energy.

In summary, we have investigated the shock compression of MOFs induced by km/s flyer plate impacts. We find that ZIF-8 crystals can maintain their crystalline structure with shocks below ≈2.5 GPa (flyer plate velocities of 0.75 km/s), but lose long-range crystalline order at ≈5 GPa (1.3 km/s) and undergo morphological changes and fragmentation. Full structural collapse with loss of local symmetry occurs with shocks ≈8 GPa (1.6 km/s). Shocks from flyer plate impacts were much more devastating to the ZIF-8 crystal morphology than quasistatic DAC compression at comparable loading pressures even with a vastly shorter exposure time (nanoseconds vs minutes). Time-resolved in situ PL and shock-induced emission indicate that the higher-velocity impacts that destroy the ZIF-8 structure also produce dramatic chemical changes and create high-energy chemical species. At least part of the excess chemical energy generated by shock-induced bond scission can be released about 50 ns later (i.e., long after the shock) in an intense emission burst. Thus, high-velocity impacts on ZIF-8 appear to be able to dissipate the energy of shock waves in two distinct ways, by the collapse of the nanoporous network and by endothermic shock-induced bond scission.

■ ASSOCIATED CONTENT

Supporting Information

The Supporting Information is available free of charge on the ACS Publications website at DOI: 10.1021/jacs.6b12956.

Experimental details, photograph of ZIF-8 films, FT-IR spectra and florescence spectra of ZIF-8 under various conditions (PDF)

■ AUTHOR INFORMATION

Corresponding Authors

*ksuslick@illinois.edu

*dlott@illinois.edu

ORCID

Kenneth S. Suslick: 0000-0001-5422-0701

Present Address

†College of Chemistry and Materials Science, Nanjing Normal University, Nanjing, China 210046

Notes

The authors declare no competing financial interest.

■ ACKNOWLEDGMENTS

The research described in this study is supported by the U.S. Office of Naval Research under award N00014-12-1-0828. This work was carried out in part in the Frederick Seitz Materials Research Laboratory Central Facilities, University of Illinois. Z.S. thanks the support from National Natural Science Foundation of China (Grant No. 21601088).

■ REFERENCES

(1) Kanel, G. I.; Razorenov, S. V.; Fortov, V. E. *Shock-Wave Phenomena and the Properties of Condensed Matter*; Springer-Verlag, 2010.

(2) (a) Kapahi, A.; Udaykumar, H. *Shock Waves* **2013**, *23*, 537−558. (b) Qiao, P. Z.; Yang, M. J.; Bobaru, F. *J. Aerosp. Eng.* **2008**, *21*, 235−248.

(3) Davison, L.; Horie, Y.; Shahinpoor, M. *High-Pressure Shock Compression of Solids IV: Response of Highly Porous Solids to Shock Loading*; Springer Science & Business Media, 2012.

(4) (a) Cherukara, M. J.; Germann, T. C.; Kober, E. M.; Strachan, A. *J. Phys. Chem. C* **2014**, *118*, 26377−26386. (b) Wood, M. A.; Cherukara, M. J.; Kober, E. M.; Strachan, A. *J. Phys. Chem. C* **2015**, *119*, 22008−22015.

(5) (a) Li, Y.; Wee, L. H.; Volodin, A.; Martens, J. A.; Vankelecom, I. F. *Chem. Commun.* **2015**, *51*, 918−920. (b) Park, K. S.; Ni, Z.; Côté, A. P.; Choi, J. Y.; Huang, R.; Uribe-Romo, F. J.; Chae, H. K.; O'Keeffe, M.; Yaghi, O. M. *Proc. Natl. Acad. Sci. U. S. A.* **2006**, *103*, 10186−10191.

(6) Su, Z.; Miao, Y.-R.; Mao, S.-M.; Zhang, G.-H.; Dillon, S.; Miller, J. T.; Suslick, K. S. *J. Am. Chem. Soc.* **2015**, *137*, 1750−1753.

(7) (a) Long, J. R.; Yaghi, O. M. *Chem. Soc. Rev.* **2009**, *38*, 1213−1214. (b) Furukawa, H.; Cordova, K. E.; O'Keeffe, M.; Yaghi, O. M. *Science* **2013**, *341*, 1230444. (c) Zhou, H.-C.; Long, J. R.; Yaghi, O. M. *Chem. Rev.* **2012**, *112*, 673−674.

(8) (a) Yot, P. G.; Vanduyfhuys, L.; Alvarez, E.; Rodriguez, J.; Itié, J.-P.; Fabry, P.; Guillou, N.; Devic, T.; Beurroies, I.; Llewellyn, P. L.; et al. *Chem. Sci.* **2016**, *7*, 446−450. (b) Howarth, A. J.; Liu, Y.; Li, P.; Li, Z.; Wang, T. C.; Hupp, J. T.; Farha, O. K. *Nature Rev. Mater.* **2016**, *1*, 15018.

(9) (a) Hu, Y.; Liu, Z.; Xu, J.; Huang, Y.; Song, Y. *J. Am. Chem. Soc.* **2013**, *135*, 9287−9290. (b) Moggach, S. A.; Bennett, T. D.; Cheetham, A. K. *Angew. Chem. Intl. Ed.* **2009**, *121*, 7221−7223.

(10) (a) Bennett, T. D.; Goodwin, A. L.; Dove, M. T.; Keen, D. A.; Tucker, M. G.; Barney, E. R.; Soper, A. K.; Bithell, E. G.; Tan, J.-C.; Cheetham, A. K. *Phys. Rev. Lett.* **2010**, *104*, 115503. (b) Tan, J. C.; Furman, J. D.; Cheetham, A. K. *J. Am. Chem. Soc.* **2009**, *131*, 14252−14254.

(11) Wei, Q.; Xu, H. W.; Yu, X. H.; Shimada, T.; Rearick, M. S.; Hickmott, D. D.; Zhao, Y. S.; Luo, S. N. *J. Appl. Phys.* **2011**, *110*, 056102.

(12) (a) Shaw, W.; Curtis, A.; Banishev, A.; Dlott, D. *J. Phys.: Conf. Ser.* **2014**, *500*, 142011. (b) Shaw, W.; Williams, R.; Dreizin, E.; Dlott, D. *J. Phys.: Conf. Ser.* **2014**, *500*, 182010. (c) Curtis, A. D.; Banishev, A. A.; Shaw, W. L.; Dlott, D. D. *Rev. Sci. Instrum.* **2014**, *85*, 043908. (d) Banishev, A. A.; Shaw, W. L.; Bassett, W. P.; Dlott, D. D. *J. Dyn. Behav. Mater.* **2016**, *2*, 194−206.

(13) (a) Bennett, T. D.; Tan, J. C.; Moggach, S. A.; Galvelis, R.; Mellot-Draznieks, C.; Reisner, B. A.; Thirumurugan, A.; Allan, D.; Cheetham, A. K. *Chem. - Eur. J.* **2010**, *16*, 10684−10690. (b) Song, Y.; Hu, D.; Liu, F.; Chen, S.; Wang, L. *Analyst* **2015**, *140*, 623−629.

(14) Hu, Y.; Kazemian, H.; Rohani, S.; Huang, Y.; Song, Y. *Chem. Commun.* **2011**, *47*, 12694−12696.

(15) Majoube, M.; Millié, P.; Vergoten, G. *J. Mol. Struct.* **1995**, *344*, 21−36.

(16) Huang, X.-C.; Li, D.; Chen, X.-M. *CrystEngComm* **2006**, *8*, 351−355.

(17) Dlott, D. D. *Annu. Rev. Phys. Chem.* **2011**, *62*, 575−597.

(18) Schmitt, D.; Svendsen, B.; Ahrens, T. J. Shock Induced Radiation from Minerals. In *Shock Waves in Condensed Matter*; Gupta, Y. M., Ed.; Plenum, 1986; pp 261−265.

DOI: 10.1021/jacs.6b12956
J. Am. Chem. Soc. XXXX, XXX, XXX−XXX